HHS Public Access

Author manuscript

Prog Retin Eye Res. Author manuscript; available in PMC 2024 July 01.

Published in final edited form as:

Prog Retin Eye Res. 2023 July ; 95: 101147. doi:10.1016/j.preteyeres.2022.101147.

Advances in understanding the molecular structure of retinoschisin while questions remain of biological function

J Bernard Heymann[1,*,†], **Camasamudram Vijayasarathy**[2,†], **Robert N Fariss**[3], **Paul A Sieving**[4]

[1]National Cryo-EM Program, Cancer Research Technology Program, Frederick National Laboratory for Cancer Research, Leidos Biomedical Research, Inc., Frederick, MD 21701, USA

[2]Section on Translational Research for Retinal and Macular Degeneration, NIDCD, NIH, Bethesda, MD 20892, U.S.A.

[3]Biological Imaging Core Facility, NEI, NIH, Bethesda, MD 20892, U.S.A.

[4]Center for Ocular Regenerative Therapy, Ophthalmology, U C Davis Health, Sacramento, CA 95817, U.S.A.

Abstract

Retinoschisin (RS1) is a secreted protein that is essential for maintaining integrity of the retina. Numerous mutations in RS1 cause X-linked retinoschisis (XLRS), a progressive degeneration of the retina that leads to vision loss in young males. A key manifestation of XLRS is the formation of cavities (cysts) in the retina and separation of the layers (schisis), disrupting synaptic transmission. There are currently no approved treatments for patients with XLRS. Strategies using adeno-associated viral (AAV) vectors to deliver functional copies of RS1 as a form of gene augmentation therapy, are under clinical evaluation. To improve therapeutic strategies for treating XLRS, it is critical to better understand the secretion of RS1 and its molecular function. Immunofluorescence and immunoelectron microscopy show that RS1 is located on the surfaces of the photoreceptor inner segments and bipolar cells. Sequence homology indicates a discoidin domain fold, similar to many other proteins with demonstrated adhesion functions. Recent structural studies revealed the tertiary structure of RS1 as two back-to-back octameric rings, each cross-linked by disulfides. The observation of higher order structures in vitro suggests the formation of an adhesive matrix spanning the distance between cells (~100 nm). Several studies indicated that RS1 readily binds to other proteins such as the sodium-potassium ATPase (NaK-ATPase) and extracellular matrix proteins. Alternatively, RS1 may influence fluid regulation

[*]Corresponding author: heymannb@mail.nih.gov.
[†]These authors contributed equally

J Bernard Heymann: Conceptualization, Investigation, Methodology, Formal analysis, Visualization, Writing - original, review, editing
Camasamudram Vijayasarathy: Conceptualization, Investigation, Writing – review, editing
Robert N Fariss: Investigation, Formal analysis, Methodology, Visualization, Writing – review, editing
Paul A Sieving: Writing – review, editing

Conflict of interest
The authors declare that they have no conflicts of interest with the contents of this article.

via interaction with membrane proteins such as the NaK-ATPase, largely inferred from the use of carbonic anhydrase inhibitors to shrink the typical intra-retinal cysts in XLRS. We discuss these models in light of RS1 structure and address the difficulty in understanding the function of RS1.

Keywords

cryo-electron microscopy; protein structure; retina; vision; fluorescence; microscopic imaging; X-linked retinoschisis; cellular adhesion; discoidin domain

1 Introduction

X-linked retinoschisis (XLRS) is characterized by the separation of retinal layers (schisis) and the formation of fluid-filled, cyst-like cavities that contribute to a gradual loss of vision (George et al., 1996; Roesch et al., 1998). XLRS is a prevalent form of inherited macular degeneration (1/25000–1/5000 (Consortium, 1998)), occurring in males beginning in young age (Sorsby et al., 1951). The cause of the disease is loss-of-function mutations in the protein retinoschisin (RS1) (Weber et al., 2002). Despite the identification of the *RS1* gene more than 20 years ago (Sauer et al., 1997) and recent studies revealing its molecular structure (Ramsay et al., 2016; Tolun et al., 2016), how RS1 maintains the integrity of the retina is still obscure. A better insight into the molecular function of RS1 will facilitate efforts to design more effective treatments for the disease.

In this review we provide some historical perspective on the clinical manifestations of XLRS and its progression in patients. Identification and cloning of the *RS1* gene, followed by sequence analysis and modeling, provided opportunities for identifying the diversity of mutations in the *RS1* gene and informing our understanding of how these mutations guide the progression of the disease. Numerous disease-causing mutations have been found throughout the sequence in XLRS patients, disrupting expression, assembly and secretion. The indication that the disease is caused by a lack of a functional RS1 protein presents an opportunity to consider gene replacement therapy. The recent determination of the molecular structure of RS1 using cryo-electron microscopy (cryoEM) clarified the consequences of many disease-causing mutations. However, most of these mutations lead to production and secretion deficiencies, leaving questions about how functional RS1 maintains the laminar structure of the retina. Improving the subcellular visualization of RS1 distribution in retina tissue by methods such as super-resolution and electron microscopy is critical to the goal of revealing its molecular function. We close on continued thoughts as to the role of RS1 in maintaining the integrity of the retina, as an adhesion molecule, or a regulator of extracellular fluid dynamics.

2 History

2.1 The disease and its diagnosis

The first description of XLRS is ascribed to Josef Haas in 1898 (Haas, 1898). It was eventually recognized as being a trait of young males with very few occurrences in females (Sorsby et al., 1951). Different terms were used to characterize the disease (George et al.,

1995) until Jager coined the term “X-linked retinoschisis” to indicate its recessive nature (Jager, 1953).

The original observations of XLRS described the presence of retinal cysts or cavities (Figure 1A) (Kleinert, 1953) that can eventually lead to retinal detachment (Mann and Macrae, 1938; Weve, 1938). While the electrical response of the retina was first reported in the nineteenth century (Holmgren, 1865), the use of the electroretinogram (ERG) in the twentieth century (Brown, 1968; Einthoven and Jolly, 1908; Riggs, 1941) presented a tool to diagnose XLRS and assess retinal function (Figure 1B). Diagnosis of XLRS during the 1950s and 1960s relied on fundoscopy (fundus examination) and ERG recording from the entire eye which reflects the total electrical activity arising from the retina in response to light stimulation. The major components of the ERG response are the a-wave ascribed to the photoreceptor depolarization, and the b-wave ascribed to the bipolar cell hyperpolarization (Brown, 1968). Optical coherence tomography (OCT) developed in the early 1990’s (Figure 1C) (Huang et al., 1991) provided a non-invasive method to reveal the cellular layers in the retina and any deviation in their structural organization.

The typical feature of the disease, present in nearly all cases, is bilateral foveal schisis (splitting), often seen as a spokewheel pattern of folds radiating out from the fovea and separation of the inner retinal layers with formation of cystic spaces in between the layers that may eventually lead to retinal detachment (Mann and Macrae, 1938; Weve, 1938). The separation of retinal layers disrupts the synaptic signal transmission from photoreceptors to bipolar cells and leads to slow, progressive loss in vision. When retinal function is assessed by ERG, many XLRS patients display a markedly reduced b-wave amplitudes compared to the a-wave, which implicates abnormal synaptic signaling or neuronal processing (Sikkink et al., 2007; Tantri et al., 2004). While the clinical aspects of XLRS vary considerably between cases, a common symptom is the reduction of the ERG b-wave (Bowles et al., 2011; Kellner et al., 1990; Tanino et al., 1985) ascribed to the response of the bipolar cells in the inner nuclear layer (INL) (Karwoski and Xu, 1999). The a-wave is variably decreased with about a third of XLRS patients falling below two standard deviations from the normal (Bowles et al., 2011).

2.2 The molecular basis of XLRS

After several studies closed in on the genetic position of XLRS (Huopaniemi et al., 1997; Weber et al., 1995), the *RS1* gene was identified on the X chromosome at p22.1 and cloned (Sauer et al., 1997). The gene consists of 6 exons and 5 introns translated into a single 224 residue protein named “retinoschisin” for the observation that many mutations in it cause the splitting of the layers in the retina. The RS1 protein features an N-terminal signal sequence required for secretion, a small unique part termed the RS1 domain, and a C-terminal conserved domain with homology to the discoidin fold. XLRS patients are typically diagnosed based on an examination of the retina and with reference to an X-linked pedigree. Genetic analysis in such patients nearly always reveals a mutation in the *RS1* gene, such as substitution, deletion, insertion, or splicing variant. Exceptions may possibly indicate regulatory elements affecting RS1 expression (Kjellstrom et al., 2010) or an intronic variation. While RS1 is mostly expressed in the retina, it is also expressed in the pineal

gland (Takada et al., 2006) and in the lung at low levels (Zhang et al., 2022), but its role in these tissues is obscure.

2.3 Mouse models and expression of retinoschisin in the retina

The monogenic nature of XLRS means that studies could focus on one protein. As with other proteins, a mouse model is useful because the murine *RS1* gene shares the same exon-intron organization and the RS1 protein has 96 % identity with the human version. Various knock-out (Liu et al., 2019; Weber et al., 2002; Zeng et al., 2004), knock-in (Chen et al., 2017) and missense mutations (Liu et al., 2019) have been introduced in mouse models. All these mouse models presented intra-retinal schisis cavities, reactive gliosis, disruption of outer plexiform (synaptic) layer, and a synaptic transmission defect seen in the ERG, all as found in the human XLRS.

Tracking *RS1* mRNA and immunohistochemistry of the developing mouse retina indicated that the production of RS1 tracks differentiation of the specialized layers (Takada et al., 2004). The different cell layers of the vertebrate retina form successively during development, starting with the innermost layer, the ganglion cell layer (GCL), followed by inner nuclear layer (INL) comprised of the bipolar, horizontal and amacrine cells, and finishing with the photoreceptors with their cell bodies in the outer nuclear layer (ONL) (Hoon et al., 2014; Reese, 2011; Stenkamp, 2015). The main glial cells of the retina, the Müller cells, differentiate last with their cell bodies located in the INL and with projections spanning the entire retina (Vecino et al., 2016). The first expression RS1, at postnatal day 1 (P1), is in the ganglion cells, with expression in other cells as they differentiate (Takada et al., 2004). Bipolar cells in the INL first label with RS1 by P7, while the ERG b-wave appears between P12 and P14 (Takada et al., 2004). At this time the photoreceptors have already established their inner and outer segments and fully expressed rhodopsin (Morrow et al., 1998). In adults, all neuronal cells express RS1, but the secreted protein is most abundant on the plasma membranes of photoreceptor inner segments and bipolar cells (Liu et al., 2019; Takada et al., 2004), with somewhat lower occurrence in the outer plexiform layer (OPL), a layer where photoreceptors form synapses with bipolar cells.

In the RS1 knockout mouse, the main structural disruption (schisis) of the retina is in or around the INL and a loss of distinction between the photoreceptor inner segment (IS) and outer segment (OS) layers (Zeng et al., 2016). Cavities form in the retina, reflecting an impairment of cell-cell adhesion (Vijayasarathy et al., 2007). Immunohistochemistry indicated the presence of RS1 in the outer plexiform layer (OPL), consistent with a role in supporting synaptic integrity (Takada et al., 2008). As in human XLRS, the knockout mice exhibit a decreased ERG b-wave (Weber et al., 2002; Zeng et al., 2004). The complexity of cyst formation is underscored by the observation that a mutation in a tyrosinase reduces schisis (Johnson et al., 2010), although a direct link to the adhesive function of RS1 is unclear.

In one $RS1^{-/y}$ model, the largest cavities occur at 4 months, decreasing in size by 16 months (Kjellstrom et al., 2007; Zeng et al., 2016), although the rate of regression varies with the specific murine $Rs1^{-/y}$ model (Vijayasarathy et al., 2021). There is a gradual loss of ERG amplitudes in knockout mice between 1 and 12 months, as well as a decrease in

photoreceptor numbers (Kjellstrom et al., 2007). Both mouse *Rs1*$^{-/y}$ models (Liu et al., 2019; Luna et al., 2009; Weber et al., 2002) and a rat *Rs1*$^{-/y}$ model (Zeng et al., 2022) show photoreceptor nuclei beyond the outer limiting membrane. In the latter case, the cysts are at maximal size at P15, but eventually collapse as the outer layers of the retina degenerate. The conclusion is that the disruption of the OPL and displacement of synaptic structures contributes considerably to the ERG changes and vision loss, becoming irreversible due to photoreceptor loss.

While rodent models are very valuable and show remarkable fidelity in mimicking human XLRS, it should be cautioned that they are significantly different from humans (Sikkink et al., 2007; Vijayasarathy et al., 2021). All the mouse models and one rat model deficient in RS1 show a similar phenotype, with both suppressed ERG a- and b- waves (Liu et al., 2019; Vijayasarathy et al., 2021; Weber et al., 2002; Zeng et al., 2004). In human XLRS patients, the responses to deficiencies in RS1 are highly variable, with two-thirds retaining a-wave amplitudes above the two-standard deviation threshold (Bowles et al., 2011). This indicates normal photoreceptor function while the main disruption is in the INL indicated by a severely depressed b-wave and cyst formation. In most of the rodent models there is no RS1 expression at all, representing a simplified experimental situation. Many of the human XLRS patients have RS1 with missense mutations that still express some of the protein, and this may account for the variability in the severity of the diseases. Although little has been inferred from the relationship between disease severity and specific mutations (Bowles et al., 2011; Sergeev et al., 2010; Sergeev et al., 2013), this may still be a factor to consider. Missense mutations have been introduced in only two mouse models, where response to the C59S mutation was milder than the R141C mutation (Liu et al., 2019). The structural consequences of the mutations are described further on.

2.4 Gene therapy

XLRS is an attractive candidate for gene augmentation therapy for several reasons: 1) loss of function is associated with one protein that can be replaced; 2) RS1 is a secreted protein that exerts its effect in the extracellular space; 3) mutations don’t cause congenital blindness and the progression is gradual so there is a window of opportunity for therapeutic intervention before neuronal death and irreversible vision loss have occurred.

Gene therapy relies on a delivery mechanism for a particular gene and an expression system to be able to produce the protein. In the case of RS1, an adeno-associated virus serotype 8 (AAV8) was chosen as a suitable delivery vector that could be packaged with the *RS1* gene and an expression promotor (for more detail, see (Vijayasarathy et al., 2021)). The ERG b-wave and retinal layering were improved in a knockout mouse treated with an AAV8 vector carrying the normal *RS1* gene (Kjellstrom et al., 2007; Ou et al., 2015; Park et al., 2009; Zeng et al., 2004). Deficiency in RS1 affected the cellular organization of synaptic proteins in the OPL such as TRPM1 and VGluT1, and these are reorganized to their proper locations with gene therapy (Ou et al., 2015). To improve specificity, an *RS1* gene-specific promotor region was engineered instead of using a non-specific promoter (Ou et al., 2015; Park et al., 2009). Because Müller cells span the retina, it was thought that they could aid in distributing RS1. However, targeting RS1 expression to the photoreceptors has a better outcome as

compared to targeting Müller cells or with a general promotor (Byrne et al., 2014). Using a bipolar specific promotor also improved retinal structure and showed distribution of RS1 to the inner segments (Vijayasarathy et al., 2022). It thus appears that secreted RS1 is properly distributed to the correct locations in the tissue for its function. Further studies in mice indicated the proper restoration of much of the synaptic machinery (Ou et al., 2015) and morphology upon AAV8-RS1 delivery (Zeng et al., 2016). Interestingly, the AAV vector size is too large to effectively penetrate the wild type retina when delivered into the vitreous cavity, while in the KO mouse the intra-retinal cavities allow entry of the viral particles (Park et al., 2009).

Gene therapy is complicated by the presence of pre-existing neutralizing antibodies against the virus vector as well as ocular inflammation as a response to an invasive procedure. Two clinical trials in XLRS patients reported a suitable safety and tolerability profile of intravitreally administered RS1 AAV vectors (Cukras et al., 2018; Pennesi et al., 2022). Dose-related ocular inflammation occurred, but this resolved with topical and oral corticosteroids. Systemic antibodies against AAV8 increased in dose-dependent fashion, but no antibodies were observed against the RS1 protein. However, neither clinical trials demonstrated a substantial treatment effect. It is thought that failure to achieve therapeutic benefit in XLRS patients is mostly related to the delivery approach, the ILM barrier to vector penetration, and the diffusion distance through the dense extracellular matrix to target photoreceptor/bipolar cells in the outer retina. The challenge is to find the correct vector-expression system combination with minimal side effects for effective therapy and effective gene delivery to the central retina (Vijayasarathy et al., 2021).

Alternative strategies have been devised that rely on delivering an expression system using nanoparticles or cells. A suitable plasmid encased in lipid nanoparticles was shown to effectively increase RS1 production in a RS1-deficient mouse model (Apaolaza et al., 2016; Apaolaza et al., 2015). A different approach is the CRISPR/Cas9-mediated knock-in of RS1 with nanoparticle vectors (Chou et al., 2020; Yang et al., 2020). Yet another method is to infiltrate the retina with mesenchymal stem cells transfected with an RS1 expression system (Bashar et al., 2016). All of these studies show some recovery of the retinal structure in mouse models, with possible translation to human therapy still in the future.

3 Structural studies

3.1 Sequence analysis, mutations and homology modeling

The 224-residue predicted sequence of RS1 has a leader peptide (signal sequence), a small unique domain (the RS1 domain), and a large C-terminal domain homologous to the discoidin domain fold (Sauer et al., 1997). This homology is seen in many other proteins (Kiedzierska et al., 2007), fostering the hope that the role of RS1 could be inferred from the common discoidin fold. However, this family of proteins have diverse functions and quaternary structures, and the relevant regions are often in the peripheral loops and surfaces. The discoidin fold therefore provides a scaffold to which the functionality is added. That means that the adhesive functions of other discoidin proteins and types of ligands binding to them are not necessarily relevant to the role of RS1.

RS1 is a highly conserved protein in eukaryotes, suggesting that it is particularly sensitive to mutation. Numerous mutations leading to XLRS are scattered throughout the RS1 sequence, with the exception of the RS1 domain. This domain is the unique part of RS1 and could be involved in a specific function. However, the lack of disease-causing mutations indicates that is likely just a vestige of evolution and has no significance in RS1.

The 23-residue leader sequence is cleaved off in the mature protein (Wu and Molday, 2003). Vijayasarathy et al. reported that, in addition, an alternative cleavage can occur after residue 21, apparently without influencing the rest of the structure (Vijayasarathy et al., 2006). Mutations in the hydrophobic core of the leader peptide (L12H and L13P) block import into the ER and lead to proteolytic degradation of synthesized RS1 in the cytoplasm (Vijayasarathy et al., 2010; Wang et al., 2002). It is therefore clear that these mutations prevent the production of a functional RS1 even before it embarks on the secretory pathway.

Disease-causing mutations are spread throughout the discoidin domain, and there is no focus on a specific sub-structure (see e.g., (Chen et al., 2020)), indicating that the structural integrity of the molecule can be compromised in many ways. The majority of mutations in the discoidin domain are retained in the ER and never exported (Gleghorn et al., 2010; Wang et al., 2002). This is likely a consequence of improper folding or assembly, which may be a requirement for secretion.

Before the structure of RS1 was determined, insight into structure-function relationships was derived from homology modeling and the numerous missense mutations. Fraternali *et al.* (Fraternali et al., 2003) constructed the first homology models of the monomer, followed by others (Sergeev et al., 2010; Sergeev et al., 2013; Wu and Liu, 2012). From these it was inferred that mutations in the core would prevent proper folding. However, the monomeric homology models could not address any possibility of oligomerization, leaving many of the disease-related mutations on the surface of the monomer without an explanation.

3.2 Targeted mutational studies show a disulfide linked octamer

Analysis of expression by reducing and non-reducing gel electrophoresis with Western blot detection indicated that RS1 is a disulfide-linked homo-oligomer (Grayson et al., 2000; Molday et al., 2001), subsequently shown to be an octamer of ~180 kDa (Wu and Molday, 2003; Wu et al., 2005). In a set of experiments, Wu et al. (Wu and Molday, 2003; Wu et al., 2005) mutated the 10 cysteines in RS1 to assess their requirement for the proper production of RS1. From these studies and using homology modeling of the discoidin domain, they concluded that C59 and C223 form inter-molecular cross-links of an octameric structure, while intra-molecular bonds are formed by C63-C219 and C110-C142 pairs. The three cysteines in the RS1 domain and the remaining C83 in the discoidin domain are not required for proper constitution of the octamer. The internal cysteine mutants (C63-C219 and C110-C142) are poorly secreted, while the C59 and C223 mutants are secreted as monomers. This indicates that at least the stabilization of the subunit by the internal disulfides is required for secretion. It is possible that the properly folded monomers assemble into octamers and are secreted, but that it dissociates easily so that we only detect monomers and perhaps dimers.

3.3 The molecular structure of retinoschisin

Three concurrent studies reported the structure of RS1: two by cryo-electron microscopy (cryoEM) at high enough resolution to allow modeling (Ramsay et al., 2016; Tolun et al., 2016), and a low-resolution structure by negative stain electron microscopy (Bush et al., 2016a). All three revealed a double-ring structure composed of two octameric rings (Figure 2A,B). Native electrophoresis confirmed the 16-mer state of the intact protein (Tolun et al., 2016). Eliminating the RS1 domain did not affect the formation of the double ring structure, indicating that it is not required for assembly (Tolun et al., 2016). The availability of the full double octamer assembly of the discoidin domain RS1 now provides a basis for understanding the effect of mutations.

The two structures of RS1 solved by cryoEM are available in the EMDB/PDB (Electron Microscopy Databank and Protein Data Bank). The first is of the wild type RS1 expressed in a baculovirus system (Tolun et al., 2016) (EMDB: 6425; PDB: 3JD6), while the second is a R141H mutant expressed in HEK cells (Ramsay et al., 2016) (EMDB: 3595; PDB: 5N6W). Because the R141H mutation is in a peripheral loop, the overall structure is very similar to the wild type (Ramsay et al., 2016). R141H is one of the rare disease-causing mutants that is fully assembled and secreted (Wang et al., 2006) but still causes XLRS (Park et al., 2000).

The resolution of these cryoEM at ~4 Å maps are relatively low, indicating a level of uncertainty in the atomic models of the RS1 discoidin domain. This is confirmed by a comparison of the two cryoEM maps by local resolution analysis that show the maps are highly similar to the limit at 4 Å (Figure 3). The discoidin fold core in each subunit is very stable as manifested by the many discoidin domain structures solved to high resolution. This means that the limitation of the resolution to 4 Å is likely due to flexibility in the octameric rings. Some of this deviation from strict symmetry was observed in higher-order assemblies (Heymann et al., 2019b). The implication is that to solve the structure to a higher resolution for better definition of the molecular details, the conformational flexibility must be addressed.

3.4 Missense mutations in the core and between subunits

The molecular structure of RS1 clarified the influence of many missense mutations that cause XLRS. In particular the roles of the disulfide cross-links are crucially important to ensure proper folding and to lock each octamer into a stable ring (Figure 2). The C59S mutant is unable to form octamers, although it is secreted as a monomer or dimer (Gleghorn et al., 2010; Wu and Molday, 2003). In contrast, the C110Y mutant forms octamers, but they are not secreted, indicating a likely folding problem leading to retention in the ER (Gleghorn et al., 2010; Wang et al., 2006).

The interactions between the octameric rings are weaker, but sufficient to preserve the double-ring structure during purification. The most prominent residues in the interface between the rings are W147 and H207 that suggests a hydrophibic interaction. A H207Q mutation that changes the polarity of the residue shows lower stability and more readily dissociates into single-ring octamers (Ramsay et al., 2016). In an organoid model of

the retina, an R209C mutant fails to produce a secreted protein while exhibiting typical retinoschisis features (Huang et al., 2019).

Many missense mutations within the core of the RS1 subunit prevent proper folding, which was originally inferred from homology modeling of the monomer (Sergeev et al., 2010; Sergeev et al., 2013; Wu and Liu, 2012). With the double-ring structure of RS1 resolved (Tolun et al., 2016), it became clear how mutations affect the interacting surfaces between subunits (Figure 2C). A prominent feature is the salt bridge between K167 on the one side, and E72 or E215 on the other side that contributes to the binding energy between subunits. Compromising any of these residues destabilizes the octamer and lead to XLRS (Chen et al., 2014; Gehrig et al., 1999; Vijayasarathy et al., 2010; Wu and Molday, 2003).

3.5 Higher order structures of RS1

Some missense mutations causing XLRS occur in the peripheral parts of the RS1 structure, indicating important interactions with other proteins. Further studies on purified RS1 showed that it can assemble into a network of filaments (Figure 4A) (Heymann et al., 2019b). Reconstruction of the main dimeric interaction in the filaments (Figure 4B) revealed the importance of the peripheral loops. One of these loops is prominent in both sides of the interface between RS1 molecules, including the aromatic residues Y89, W92, and Y93 (Figures 2C and 4C). Mutations in these residues cause disease, suggesting that higher order assembly may have a role in RS1 function. Such a network may provide an important scaffold for other proteins in the intercellular matrix. This is supported by the implication of some peripheral mutations in interactions with other proteins, such as the abundant NaK-ATPase (Plossl et al., 2018).

3.6 Assembly and secretion

With 3D structures of RS1 and a long list of influential mutations, we can now formulate a better picture of RS1 production. It was recognized early on that many of the mutants are retained in the ER (Wang et al., 2002; Wu and Molday, 2003);Gleghorn, 2010 #4672; (Sudha et al., 2018). A pulse-chase study indicated that the wild-type RS1 octamer is already formed in the ER (Gleghorn et al., 2010). Most of the mutants therefore result in a null-phenotype, with no secretion of even a partially functional protein. Even in the cases where an RS1 mutant is secreted, it does not appear to affect the severity of the disease (Sudha et al., 2018). This means that RS1 must be produced and secreted as the double ring 16-mer as a minimum requirement.

Nevertheless, there are some studies reporting the secretion of monomers or dimers, such as the E72K mutant (Vijayasarathy et al., 2010) and the C59S mutant (Dyka and Molday, 2007; Gleghorn et al., 2010; Liu et al., 2019; Skorczyk and Krawczynski, 2012; Wang et al., 2006; Wu and Molday, 2003). The dimer in the C59S-C223S double mutant is ascribed to cross-linking the C40 of the RS1 domain (Wu et al., 2005). This may be related to the diffuse appearance of the RS1 domain in the cryoEM maps (Figure 2A). The occurrence of three cysteines in the RS1 domain provides an opportunity for variation in the cross-linking between subunits and a somewhat disorganized structure. A mouse with the C59S mutation exhibited a less severe phenotype, suggesting that the mutation is not as disruptive as for

typical XLRS. (Liu et al., 2019). While this may indicate the dimer can provide some functionality, it is more likely that the mutant RS1 still assembles to some extent as the full 16-mer.

Some missense mutants are fully assembled and secreted. These include two mutants associated with the connections between the rings, H207Q and R209H (Plossl et al., 2018). Mutations at R141 have various consequences, with conversion to A/G/H/S fully assembled and secreted, and others not secreted at all (C/E/K/Q/V) (Dyka and Molday, 2007; Heymann et al., 2019b; Plossl et al., 2018; Sudha et al., 2018; Wang et al., 2002; Wang et al., 2006; Wu and Molday, 2003). Presumably some conformational changes preclude the fully assembled and secreted RS1 from interacting with partners necessary to avoid causing the disease.

Once secreted, RS1 appears to remain bound to the cell membrane (Vijayasarathy et al., 2007; Wang et al., 2006). It is strongly localized on the photoreceptor inner segment and bipolar cells (Figures 5,6), while completely absent from the outer segment (Vijayasarathy et al., 2007). The simplest explanation is that it retains its interaction with the membrane and/or proteins while being secreted. However, in gene therapy experiments where the expression may not be confined to the photoreceptors and bipolar cells, RS1 still localized to the photoreceptors (Zeng et al., 2016).

4 RS1 location within the retinal morphology

RS1 is mainly expressed in photoreceptor and bipolar cells (Molday et al., 2001). Along with other photoreceptor proteins, RS1 is also expressed in the pineal gland (Takada et al., 2006), although this may reflect a pattern of expression by a population of vestigial neurons with photoreceptor-like qualities. Labeling RS1 in the mouse retina with fluorescent antibodies shows expression on the outer surface of the membranes of the photoreceptor inner segments (Figure 5 & Figure 6A) and the bipolar cells (Figure 5 & Figure 6B). The main rupture of the retina to produce the characteristic cysts occurs in the INL, but the photoreceptors can also separate in the mouse model (Vijayasarathy et al., 2007). In children with an early onset of the diseases, the largest cysts occur in the INL of most eyes, with smaller cysts in the ONL and OPL (the nuclear and synaptic parts of the photoreceptors) (Ling et al., 2020).

XLRS was originally theorized as a defect of Müller cells (Kirsch et al., 1996; Sauer et al., 1997). Müller cells are the principal glial cells that span the retina and are important in fluid homeostasis and for structural support (Bringmann and Wiedemann, 2012). When retinal integrity is compromised, Müller cells demonstrate a profound capacity for hypertrophy. A $RS1^{-/y}$ knockout mouse exhibits severe retinal trauma associated with upregulation of the glial fibrillary acidic protein (GFAP) in the Müller cells and extrusion of photoreceptors into the subretinal space (Luna et al., 2009). Gene therapy experiments in a knockout mouse showed that expression from Müller cells can be engineered, but that it is not as restorative as expression from photoreceptors (Byrne et al., 2014). These findings suggest that the Müller cells are not primarily involved in the function of RS1 but contribute to the degeneration of retinal integrity.

A likely role for Müller cells is in regulating fluid movement and intraretinal pressure, in particular the highly expressed water channel, AQP4, potassium channel, Kir4.1 (Nagelhus et al., 2004) and carbonic anhydrase XIV (Nagelhus et al., 2005; Ochrietor et al., 2005). The latter is coupled to XLRS by the observation that carbonic anhydrase inhibitors such as dorzolamide (Khandhadia et al., 2011; Walia et al., 2009) and acetazolamide (Collison and Fishman, 2016; Verbakel et al., 2016) are able to reduce the volume of the cysts and relieve some of the symptoms of the disease. The response to these inhibitors is highly variable, with some patients experiencing a recurrence of cysts (Ambrosio et al., 2021; Andreuzzi et al., 2017). When the normal adhesion mechanisms are absent, as in XLRS, the hypertrophy of Müller cells may contribute to a positive feedback scenario driven by their disfunction and gliosis.

5 What is the molecular function of RS1?

Studying the function of RS1 is problematic because its effect is binary: it is either properly produced and secreted in a functional form or not. Thus, the numerous mutations causing XLRS make it difficult to target specific parts of the structure. The mouse gene therapy worked whether the RS1 was expressed widely or with a specific promotor limiting it to the photoreceptors (Bush et al., 2016b; Ou et al., 2015; Park et al., 2009) or the bipolar cells (Vijayasarathy et al., 2022). In all these cases the ERG b-wave amplitude recovered, and cavity size decreased, whereas the inner segments and bipolar cells were extensively coated with RS1. Therefore, the conclusion is that the secreted RS1 is somehow targeted to the correct locations in the retina. This may be attributed to a binding partner, either already on the cell surface, or co-expressed and co-secreted with RS1.

The consequence of the inability to produce and secrete a functional RS1 leads to the defining structural character of XLRS, separation of the retinal layers and the formation of cysts. Possible mechanisms by which this can occur are inadequate adhesion or excessive intercellular pressure, or both. XLRS usually develops gradually in young males in most cases, suggesting that RS1 is not critically involved in the formation of the retina but rather supports its integrity throughout life. However, in retinal organoids, Huang et al. (Huang et al., 2019) provides evidence that the formation of the retina depends on proper RS1 expression. Perhaps both mechanisms contribute to XLRS, with the lack of adhesion manifesting when the extracellular pressure increases. This would explain relief of structural pathology reported with the use of carbonic anhydrase inhibitors.

The hope was that with resolving the structure of RS1, we would understand how it functions as an adhesive molecule. However, most recognized cell-cell adhesion molecules have a transmembrane domain (Chothia and Jones, 1997; Honig and Shapiro, 2020), but RS1 does not have an obvious membrane insertion domain such as a hydrophobic or amphipathic helix. However, RS1 has very hydrophic residues in the protruding loops on the periphery of the double ring structure, proposed to interact with membranes (Fraternali et al., 2003). It also copurifies with membrane fractions (Vijayasarathy et al., 2007). The adherence of purified RS1 filaments to the hydrophobic air-water interface as observed by cryoEM (Heymann et al., 2019b) further supports the peripheral loops as the interacting

surfaces. Visualizing RS1 in the retina may resolve this issue, although with daunting challenges.

The interaction of RS1 with other proteins may have both structural and functional attributes. One potential partner for RS1 interaction that has been suggested is the NaK-ATPase, which is abundant on plasma membranes in several classes of retinal neurons. It was reported to bind to RS1, an interaction that may indicate a regulatory function (Plossl et al., 2017a; Plossl et al., 2017b). The most abundant retinal NaK-ATPase consists of ATP1-A3 and ATP1-B2. RS1 was shown to bind to residue T240 in ATP1-B2 (Plossl et al., 2019). A recent study found that cardiac glycosides, potent inhibitors of the pump function of NaK-ATPase, can displace RS1 (Schmid et al., 2020). However, the cardiac glycosides do not compete for the same binding site, suggesting an allosteric mechanism. This further complicates the function of RS1, as it is likely an integral part of the intercellular matrix of the retina, potentially interacting with numerous other proteins.

Over the course of XLRS in the mouse knockout model, the early retina appears intact as assessed by OCT, with the cyst sizes increasing up to the third or fourth month, but then decreasing to the point where the retina resembles its wild type counterpart (Zeng et al., 2016; Zhour et al., 2012). This indicates that the factors that underly fluid buildup dissipates, although the decrease in the schisis does not correlate with restoration of electrophysiological function. Perhaps the strongest evidence for pressure control comes from the use of carbonic anhydrase inhibitors (Collison and Fishman, 2016; Khandhadia et al., 2011; Verbakel et al., 2016; Walia et al., 2009) to shrink the cysts and possibly recover some function. However, the disruption of the retinal organization is extensive (Luna et al., 2009) and the recoveries are rather moderate. Therefore, the use of carbonic anhydrase inhibitors is a treatment for the symptoms of XLRS but it does not resolve any underlying pathology. A normal-looking retina may still have deficiencies that are only evident at a molecular level.

The unique structural features of RS1 may mean that it functions as an adhesion protein to maintain the integrity of the retinal layers, but it allows the retina to be flexible enough to tolerate fluid fluctuations without disintegrating. OCT shows that the subretinal space expands and contracts several microns due to fluid flux driven by light conditions (Li et al., 2016). Similarly, two-photon imaging revealed that light stimulation rapidly decreases the extracellular space in the mouse IPL (Kuo et al., 2020). Such dynamism requires an elastic adhesion between cells and not the rigid structure of other junctions.

6 Conclusion

While we hoped that the structure of RS1 would shed light on its function, it has settled some questions about mutants but left us with much more to ponder. Part of the frustration is that it is a very unique protein mainly of the retina with little to no expression in other tissues. What would it take to clarify its function? The first task is to examine its locations on and interactions with the cellular surface within the context of retinal tissue at a sufficient resolution to see individual molecules (Heymann et al., 2019a). Another task is to better define its interaction partners through mutational analysis coupled with co-localization and

visualization. Furthermore, the point at which the molecule is properly folded and assembled should be established, potentially also identifying early interactions with other proteins.

Abbreviations:

XLRS	X-linked retinoschisis
RS1	retinoschisin
CryoEM	Cryo-electron microscopy
OCT	optical coherence tomography
ERG	electroretinogram
GCL	Ganglion cell layer
INL	Inner nuclear layer
ONL	Outer nuclear layer
IPL	Inner plexiform layer
OPL	Outer plexiform layer
IS	Inner segment of the photoreceptor
OS	Outer segment of the photoreceptor
NaK-ATPase	Sodium potassium adenosine triphosphatase
AAV	Adeno-associated virus
RS1$^{-/y}$	Referring to a mouse model with a deficient RS1 gene on the X-chromosome

References

Ambrosio L, Williams JS, Gutierrez A, Swanson EA, Munro RJ, Ferguson RD, Fulton AB, Akula JD, 2021. Carbonic anhydrase inhibition in X-linked retinoschisis: An eye on the photoreceptors. Exp Eye Res 202, 108344.

Andreuzzi P, Fishman GA, Anderson RJ, 2017. Use Of A Carbonic Anhydrase Inhibitor In X-Linked Retinoschisis: Effect on Cystic-Appearing Macular Lesions and Visual Acuity. Retina 37, 1555–1561. [PubMed: 27828908]

Apaolaza PS, Del Pozo-Rodriguez A, Solinis MA, Rodriguez JM, Friedrich U, Torrecilla J, Weber BH, Rodriguez-Gascon A, 2016. Structural recovery of the retina in a retinoschisin-deficient mouse after gene replacement therapy by solid lipid nanoparticles. Biomaterials 90, 40–49. [PubMed: 26986855]

Apaolaza PS, Del Pozo-Rodriguez A, Torrecilla J, Rodriguez-Gascon A, Rodriguez JM, Friedrich U, Weber BH, Solinis MA, 2015. Solid lipid nanoparticle-based vectors intended for the treatment of X-linked juvenile retinoschisis by gene therapy: In vivo approaches in Rs1h-deficient mouse model. J Control Release 217, 273–283. [PubMed: 26400864]

Bashar AE, Metcalfe AL, Viringipurampeer IA, Yanai A, Gregory-Evans CY, Gregory-Evans K, 2016. An ex vivo gene therapy approach in X-linked retinoschisis. Mol Vis 22, 718–733. [PubMed: 27390514]

Bowles K, Cukras C, Turriff A, Sergeev Y, Vitale S, Bush RA, Sieving PA, 2011. X-linked retinoschisis: RS1 mutation severity and age affect the ERG phenotype in a cohort of 68 affected male subjects. Invest Ophthalmol Vis Sci 52, 9250–9256. [PubMed: 22039241]

Bringmann A, Wiedemann P, 2012. Muller glial cells in retinal disease. Ophthalmologica 227, 1–19.

Brown KT, 1968. The eclectroretinogram: its components and their origins. Vision Res 8, 633–677. [PubMed: 4978009]

Bush M, Setiaputra D, Yip CK, Molday RS, 2016a. Cog-Wheel Octameric Structure of RS1, the Discoidin Domain Containing Retinal Protein Associated with X-Linked Retinoschisis. PLoS One 11, e0147653.

Bush RA, Zeng Y, Colosi P, Kjellstrom S, Hiriyanna S, Vijayasarathy C, Santos M, Li J, Wu Z, Sieving PA, 2016b. Preclinical Dose-Escalation Study of Intravitreal AAV-RS1 Gene Therapy in a Mouse Model of X-linked Retinoschisis: Dose-Dependent Expression and Improved Retinal Structure and Function. Hum Gene Ther 27, 376–389. [PubMed: 27036983]

Byrne LC, Ozturk BE, Lee T, Fortuny C, Visel M, Dalkara D, Schaffer DV, Flannery JG, 2014. Retinoschisin gene therapy in photoreceptors, Muller glia or all retinal cells in the Rs1h−/−mouse. Gene Ther 21, 585–592. [PubMed: 24694538]

Chen CJ, Xie Y, Sun TY, Tian L, Xu K, Zhang XH, Li Y, 2020. Clinical findings and RS1 genotype in 90 Chinese families with X-linked retinoschisis. Molecular Vision 26, 291–298. [PubMed: 32300273]

Chen D, Xu T, Tu M, Xu J, Zhou C, Cheng L, Yang R, Yang T, Zheng W, He X, Deng R, Ge X, Li J, Song Z, Zhao J, Gu F, 2017. Recapitulating X-Linked Juvenile Retinoschisis in Mouse Model by Knock-In Patient-Specific Novel Mutation. Front Mol Neurosci 10, 453. [PubMed: 29379415]

Chen J, Xu K, Zhang X, Pan Z, Dong B, Li Y, 2014. Novel mutations of the RS1 gene in a cohort of Chinese families with X-linked retinoschisis. Mol Vis 20, 132–139. [PubMed: 24505212]

Chothia C, Jones EY, 1997. The molecular structure of cell adhesion molecules. Annu Rev Biochem 66, 823–862. [PubMed: 9242926]

Chou S-J, Yang P, Ban Q, Yang Y-P, Wang M-L, Chien C-S, Chen S-J, Sun N, Zhu Y, Liu H, Hui W, Lin T-C, Wang F, Zhang RY, Nguyen VQ, Liu W, Chen M, Jonas SJ, Weiss PS, Tseng H-R, Chiou S-H, 2020. Dual Supramolecular Nanoparticle Vectors Enable CRISPR/Cas9-Mediated Knockin of Retinoschisin 1 Gene—A Potential Nonviral Therapeutic Solution for X-Linked Juvenile Retinoschisis. Advanced Science 7, 1903432.

Collison FT, Fishman GA, 2016. Structural and Functional Monitoring of Extramacular Cystoid Spaces in a Case of X-Linked Retinoschisis Treated with Acetazolamide. Retin Cases Brief Rep 12(4), 318–321.

Consortium, T.R., 1998. Functional implications of the spectrum of mutations found in 234 cases with X-linked juvenile retinoschisis.. Hum Mol Genet 7, 1185–1192. [PubMed: 9618178]

Cukras C, Wiley HE, Jeffrey BG, Sen HN, Turriff A, Zeng Y, Vijayasarathy C, Marangoni D, Ziccardi L, Kjellstrom S, Park TK, Hiriyanna S, Wright JF, Colosi P, Wu Z, Bush RA, Wei LL, Sieving PA, 2018. Retinal AAV8-RS1 Gene Therapy for X-Linked Retinoschisis: Initial Findings from a Phase I/IIa Trial by Intravitreal Delivery. Mol Ther 26, 2282–2294. [PubMed: 30196853]

Dyka FM, Molday RS, 2007. Coexpression and interaction of wild-type and missense RS1 mutants associated with X-linked retinoschisis: its relevance to gene therapy. Invest Ophthalmol Vis Sci 48, 2491–2497. [PubMed: 17525175]

Einthoven W, Jolly WA, 1908. The form and magnitude of the electrical response of the eye to stimulation by light at various intensities. Quarterly Journal of Experimental Physiology 1, 373–416.

Fraternali F, Cavallo L, Musco G, 2003. Effects of pathological mutations on the stability of a conserved amino acid triad in retinoschisin. FEBS Lett 544, 21–26. [PubMed: 12782284]

Gehrig A, White K, Lorenz B, Andrassi M, Clemens S, Weber BH, 1999. Assessment of RS1 in X-linked juvenile retinoschisis and sporadic senile retinoschisis. Clin Genet 55, 461–465. [PubMed: 10450864]

George NDL, Yates JRW, Moore AT, 1995. X-Linked Retinoschisis. British Journal of Ophthalmology 79, 697–702. [PubMed: 7662639]

George NDL, Yates JRW, Moore AT, 1996. Clinical features in affected males with X-linked retinoschisis. Archives of Ophthalmology 114, 274–280. [PubMed: 8600886]

Gleghorn LJ, Trump D, Bulleid NJ, 2010. Wild-type and missense mutants of retinoschisin co-assemble resulting in either intracellular retention or incorrect assembly of the functionally active octamer. Biochem J 425, 275–283.

Grayson C, Reid SN, Ellis JA, Rutherford A, Sowden JC, Yates JR, Farber DB, Trump D, 2000. Retinoschisin, the X-linked retinoschisis protein, is a secreted photoreceptor protein, and is expressed and released by Weri-Rb1 cells. Hum Mol Genet 9, 1873–1879. [PubMed: 10915776]

Haas J, 1898. Ueber das Zusammenvorkommen von Veränderungen der Retina und Chorioidea. Archiv für Augenheilkunde 37, 343–348.

Heymann JB, Bleck CKE, Fariss RN, Vijayasarathy C, Winkler DC, Huang R, Dearborn AD, Smirnov A, Sieving PA, Steven AC, 2019a. Hunting for the Adhesion Molecule, Retinoschisin, in Retina using CEMOVIS. Microscopy and Microanalysis 25, 1308–1309.

Heymann JB, Vijayasarathy C, Huang RK, Dearborn AD, Sieving PA, Steven AC, 2019b. Cryo-EM of retinoschisin branched networks suggests an intercellular adhesive scaffold in the retina. J Cell Biol 218, 1027–1038. [PubMed: 30630865]

Holmgren F, 1865. Method att objectivera effecten af ljusintryck på retina. Upsala Lakareforenings Forhandlingar 1, 177–191.

Honig B, Shapiro L, 2020. Adhesion Protein Structure, Molecular Affinities, and Principles of Cell-Cell Recognition. Cell 181, 520–535. [PubMed: 32359436]

Hoon M, Okawa H, Della Santina L, Wong ROL, 2014. Functional architecture of the retina: Development and disease. Progress in Retinal and Eye Research 42, 44–84. [PubMed: 24984227]

Huang D, Swanson EA, Lin CP, Schuman JS, Stinson WG, Chang W, Hee MR, Flotte T, Gregory K, Puliafito CA, Fujimoto JG, 1991. Optical Coherence Tomography. Science 254, 1178–1181. [PubMed: 1957169]

Huang KC, Wang ML, Chen SJ, Kuo JC, Wang WJ, Nhi Nguyen PN, Wahlin KJ, Lu JF, Tran AA, Shi M, Chien Y, Yarmishyn AA, Tsai PH, Yang TC, Jane WN, Chang CC, Peng CH, Schlaeger TM, Chiou SH, 2019. Morphological and Molecular Defects in Human Three-Dimensional Retinal Organoid Model of X-Linked Juvenile Retinoschisis. Stem Cell Reports 13, 906–923. [PubMed: 31668851]

Huopaniemi L, Rantala A, Tahvanainen E, de la Chapelle A, Alitalo T, 1997. Linkage disequilibrium and physical mapping of X-linked juvenile retinoschisis. Am J Hum Genet 60, 1139–1149. [PubMed: 9150161]

Jager GM, 1953. A Hereditary Affection of the Retina. Ophthalmologica 125, 470–471.

Johnson BA, Cole BS, Geisert EE, Ikeda S, Ikeda A, 2010. Tyrosinase is the modifier of retinoschisis in mice. Genetics 186, 1337–1344. [PubMed: 20876567]

Karwoski CJ, Xu X, 1999. Current source-density analysis of light-evoked field potentials in rabbit retina. Vis Neurosci 16, 369–377. [PubMed: 10367970]

Kellner U, Brummer S, Foerster MH, Wessing A, 1990. X-linked congenital retinoschisis. Graefes Arch Clin Exp Ophthalmol 228, 432–437. [PubMed: 2227486]

Khandhadia S, Trump D, Menon G, Lotery AJ, 2011. X-linked retinoschisis maculopathy treated with topical dorzolamide, and relationship to genotype. Eye (Lond) 25, 922–928. [PubMed: 21527955]

Kiedzierska A, Smietana K, Czepczynska H, Otlewski J, 2007. Structural similarities and functional diversity of eukaryotic discoidin-like domains. Biochim Biophys Acta 1774, 1069–1078. [PubMed: 17702679]

Kirsch LS, Brownstein S, de Wolff-Rouendaal D, 1996. A histopathological, ultrastructural and immunohistochemical study of congenital hereditary retinoschisis. Can J Ophthalmol 31, 301–310. [PubMed: 8913633]

Kjellstrom S, Bush RA, Zeng Y, Takada Y, Sieving PA, 2007. Retinoschisin gene therapy and natural history in the Rs1h-KO mouse: long-term rescue from retinal degeneration. Invest Ophthalmol Vis Sci 48, 3837–3845. [PubMed: 17652759]

Kjellstrom S, Vijayasarathy C, Ponjavic V, Sieving PA, Andreasson S, 2010. Long-term 12 year follow-up of X-linked congenital retinoschisis. Ophthalmic Genet 31, 114–125. [PubMed: 20569020]

Kleinert H, 1953. Eine recessiv-geschlechtsgebundene Form der idiopathischen Netzhautspaltung bei nichtmyopen Jugendlichen. Albrecht Von Graefes Arch Ophthalmol 154, 295–305. [PubMed: 13124228]

Kuo SP, Chiang PP, Nippert AR, Newman EA, 2020. Spatial Organization and Dynamics of the Extracellular Space in the Mouse Retina. J Neurosci 40, 7785–7794. [PubMed: 32887746]

Li Y, Fariss RN, Qian JW, Cohen ED, Qian H, 2016. Light-Induced Thickening of Photoreceptor Outer Segment Layer Detected by Ultra-High Resolution OCT Imaging. Invest Ophthalmol Vis Sci 57, OCT105–111.

Ling KP, Mangalesh S, Tran-Viet D, Gunther R, Toth CA, Vajzovic L, 2020. Handheld Spectral Domain Optical Coherence Tomography Findings of X-Linked Retinoschisis in Early Childhood. Retina 40, 1996–2003. [PubMed: 31764609]

Liu Y, Kinoshita J, Ivanova E, Sun D, Li H, Liao T, Cao J, Bell BA, Wang JM, Tang Y, Brydges S, Peachey NS, Sagdullaev BT, Romano C, 2019. Mouse models of X-linked juvenile retinoschisis have an early onset phenotype, the severity of which varies with genotype. Hum Mol Genet 28, 3072–3090. [PubMed: 31174210]

Luna G, Kjellstrom S, Verardo MR, Lewis GP, Byun J, Sieving PA, Fisher SK, 2009. The effects of transient retinal detachment on cavity size and glial and neural remodeling in a mouse model of X-linked retinoschisis. Invest Ophthalmol Vis Sci 50, 3977–3984. [PubMed: 19387072]

Mann I, Macrae A, 1938. Congenital Vascular Veils in the Vitreous. Br J Ophthalmol 22, 1–10. [PubMed: 18169498]

Molday LL, Hicks D, Sauer CG, Weber BH, Molday RS, 2001. Expression of X-linked retinoschisis protein RS1 in photoreceptor and bipolar cells. Invest Ophthalmol Vis Sci 42, 816–825. [PubMed: 11222545]

Morrow EM, Belliveau MJ, Cepko CL, 1998. Two phases of rod photoreceptor differentiation during rat retinal development. J Neurosci 18, 3738–3748. [PubMed: 9570804]

Nagelhus EA, Mathiisen TM, Bateman AC, Haug FM, Ottersen OP, Grubb JH, Waheed A, Sly WS, 2005. Carbonic anhydrase XIV is enriched in specific membrane domains of retinal pigment epithelium, Muller cells, and astrocytes. Proc Natl Acad Sci U S A 102, 8030–8035. [PubMed: 15901897]

Nagelhus EA, Mathiisen TM, Ottersen OP, 2004. Aquaporin-4 in the central nervous system: cellular and subcellular distribution and coexpression with KIR4.1. Neuroscience 129, 905–913. [PubMed: 15561407]

Ochrietor JD, Clamp MF, Moroz TP, Grubb JH, Shah GN, Waheed A, Sly WS, Linser PJ, 2005. Carbonic anhydrase XIV identified as the membrane CA in mouse retina: strong expression in Muller cells and the RPE. Exp Eye Res 81, 492–500. [PubMed: 16126196]

Ou J, Vijayasarathy C, Ziccardi L, Chen S, Zeng Y, Marangoni D, Pope JG, Bush RA, Wu Z, Li W, Sieving PA, 2015. Synaptic pathology and therapeutic repair in adult retinoschisis mouse by AAV-RS1 transfer. J Clin Invest 125(7), 2891–2903. [PubMed: 26098217]

Park JH, Ott SH, Wang X, Appukuttan B, Patel RJ, Van Boemel GB, Stout JT, 2000. Clinical phenotype associated with the arg141 his mutation in the X-linked retinoschisis gene. Arch Ophthalmol 118, 127–129. [PubMed: 10636429]

Park TK, Wu Z, Kjellstrom S, Zeng Y, Bush RA, Sieving PA, Colosi P, 2009. Intravitreal delivery of AAV8 retinoschisin results in cell type-specific gene expression and retinal rescue in the Rs1-KO mouse. Gene Ther 16, 916–926. [PubMed: 19458650]

Pennesi ME, Yang P, Birch DG, Weng CY, Moore AT, Iannaccone A, Comander JI, Jayasundera T, Chulay J, Group X-S, 2022. Intravitreal Delivery of rAAV2tYF-CB-hRS1 Vector for Gene Augmentation Therapy in Patients with X-Linked Retinoschisis: 1-Year Clinical Results. Ophthalmol Retina.

Plossl K, Royer M, Bernklau S, Tavraz NN, Friedrich T, Wild J, Weber BHF, Friedrich U, 2017a. Retinoschisin is linked to retinal Na/K-ATPase signaling and localization. Mol Biol Cell 28(16), 2178–2189. [PubMed: 28615319]

Plossl K, Schmid V, Straub K, Schmid C, Ammon M, Merkl R, Weber BHF, Friedrich U, 2018. Pathomechanism of mutated and secreted retinoschisin in X-linked juvenile retinoschisis. Exp Eye Res 177, 23–34. [PubMed: 30040949]

Plossl K, Straub K, Schmid V, Strunz F, Wild J, Merkl R, Weber BHF, Friedrich U, 2019. Identification of the retinoschisin-binding site on the retinal Na/K-ATPase. PLoS One 14, e0216320.

Plossl K, Weber BH, Friedrich U, 2017b. The X-linked juvenile retinoschisis protein retinoschisin is a novel regulator of mitogen-activated protein kinase signalling and apoptosis in the retina. J Cell Mol Med 21, 768–780. [PubMed: 27995734]

Ramsay EP, Collins RF, Owens TW, Siebert CA, Jones RPO, Wang T, Roseman AM, Baldock C, 2016. Structural analysis of X-linked retinoschisis mutations reveals distinct classes which differentially effect retinoschisin function. Hum Mol Genet 25, 5311–5320. [PubMed: 27798099]

Reese BE, 2011. Development of the retina and optic pathway. Vision Research 51, 613–632. [PubMed: 20647017]

Riggs LA, 1941. Continuous and reproducible records of the electrical activity of the human retina. Proceedings of the Society for Experimental Biology and Medicine 48, 204–207.

Roesch MT, Ewing CC, Gibson AE, Weber BH, 1998. The natural history of X-linked retinoschisis. Can J Ophthalmol 33, 149–158. [PubMed: 9606571]

Sauer CG, Gehrig A, Warneke-Wittstock R, Marquardt A, Ewing CC, Gibson A, Lorenz B, Jurklies B, Weber BH, 1997. Positional cloning of the gene associated with X-linked juvenile retinoschisis. Nat Genet 17, 164–170. [PubMed: 9326935]

Schmid V, Plossl K, Schmid C, Bernklau S, Weber BHF, Friedrich U, 2020. Retinoschisin and Cardiac Glycoside Crosstalk at the Retinal Na/K-ATPase. Invest Ophthalmol Vis Sci 61, 1.

Sergeev YV, Caruso RC, Meltzer MR, Smaoui N, MacDonald IM, Sieving PA, 2010. Molecular modeling of retinoschisin with functional analysis of pathogenic mutations from human X-linked retinoschisis. Hum Mol Genet 19, 1302–1313. [PubMed: 20061330]

Sergeev YV, Vitale S, Sieving PA, Vincent A, Robson AG, Moore AT, Webster AR, Holder GE, 2013. Molecular modeling indicates distinct classes of missense variants with mild and severe XLRS phenotypes. Hum Mol Genet 22, 4756–4767. [PubMed: 23847049]

Sikkink SK, Biswas S, Parry NR, Stanga PE, Trump D, 2007. X-linked retinoschisis: an update. J Med Genet 44, 225–232. [PubMed: 17172462]

Skorczyk A, Krawczynski MR, 2012. Four novel RS1 gene mutations in Polish patients with X-linked juvenile retinoschisis. Mol Vis 18, 3004–3012. [PubMed: 23288992]

Sorsby A, Klein M, Gann JH, Siggins G, 1951. Unusual retinal detachment possibly sex-linked. Br J Ophthalmol 35, 1–10. [PubMed: 14821274]

Stenkamp D, 2015. Development of the Vertebrate Eye and Retina. Progress in molecular biology and translational science 134, 397–414. [PubMed: 26310167]

Sudha D, Neriyanuri S, Sachidanandam R, Natarajan SN, Gandra M, Tharigopala A, Sivashanmugam M, Alameen M, Vetrivel U, Gopal L, Khetan V, Raman R, Sen P, Chidambaram S, Arunachalam JP, 2018. Understanding variable disease severity in X-linked retinoschisis: Does RS1 secretory mechanism determine disease severity? PLoS One 13, e0198086.

Takada Y, Fariss RN, Muller M, Bush RA, Rushing EJ, Sieving PA, 2006. Retinoschisin expression and localization in rodent and human pineal and consequences of mouse RS1 gene knockout. Mol Vis 12, 1108–1116. [PubMed: 17093404]

Takada Y, Fariss RN, Tanikawa A, Zeng Y, Carper D, Bush R, Sieving PA, 2004. A retinal neuronal developmental wave of retinoschisin expression begins in ganglion cells during layer formation. Invest Ophthalmol Vis Sci 45, 3302–3312. [PubMed: 15326155]

Takada Y, Vijayasarathy C, Zeng Y, Kjellstrom S, Bush RA, Sieving PA, 2008. Synaptic pathology in retinoschisis knockout (Rs1−/y) mouse retina and modification by rAAV-Rs1 gene delivery. Invest Ophthalmol Vis Sci 49, 3677–3686. [PubMed: 18660429]

Tanino T, Katsumi O, Hirose T, 1985. Electrophysiological similarities between two eyes with X-linked recessive retinoschisis. Doc Ophthalmol 60, 149–161. [PubMed: 4042821]

Tantri A, Vrabec TR, Cu-Unjieng A, Frost A, Annesley WH Jr., Donoso LA, 2004. X-linked retinoschisis: a clinical and molecular genetic review. Surv Ophthalmol 49, 214–230. [PubMed: 14998693]

Tolun G, Vijayasarathy C, Huang R, Zeng Y, Li Y, Steven AC, Sieving PA, Heymann JB, 2016. Paired octamer rings of retinoschisin suggest a junctional model for cell-cell adhesion in the retina. Proc Natl Acad Sci U S A 113, 5287–5292. [PubMed: 27114531]

Vecino E, Rodriguez FD, Ruzafa N, Pereiro X, Sharma SC, 2016. Glia–neuron interactions in the mammalian retina. Progress in Retinal and Eye Research 51, 1–40. [PubMed: 26113209]

Veleri S, Nellissery J, Mishra B, Manjunath SH, Brooks MJ, Dong L, Nagashima K, Qian H, Gao C, Sergeev YV, Huang XF, Qu J, Lu F, Cideciyan AV, Li T, Jin ZB, Fariss RN, Ratnapriya R, Jacobson SG, Swaroop A, 2017. REEP6 mediates trafficking of a subset of Clathrin-coated vesicles and is critical for rod photoreceptor function and survival. Hum Mol Genet 26, 2218–2230. [PubMed: 28369466]

Verbakel SK, van de Ven JP, Le Blanc LM, Groenewoud JM, de Jong EK, Klevering BJ, Hoyng CB, 2016. Carbonic Anhydrase Inhibitors for the Treatment of Cystic Macular Lesions in Children With X-Linked Juvenile Retinoschisis. Invest Ophthalmol Vis Sci 57, 5143–5147. [PubMed: 27699410]

Vijayasarathy C, Gawinowicz MA, Zeng Y, Takada Y, Bush RA, Sieving PA, 2006. Identification and characterization of two mature isoforms of retinoschisin in murine retina. Biochem Biophys Res Commun 349, 99–105. [PubMed: 16930543]

Vijayasarathy C, Sardar Pasha SPB, Sieving PA, 2021. Of men and mice: Human X-linked retinoschisis and fidelity in mouse modeling. Prog Retin Eye Res, 100999.

Vijayasarathy C, Sui R, Zeng Y, Yang G, Xu F, Caruso RC, Lewis RA, Ziccardi L, Sieving PA, 2010. Molecular mechanisms leading to null-protein product from retinoschisin (RS1) signal-sequence mutants in X-linked retinoschisis (XLRS) disease. Hum Mutat 31, 1251–1260. [PubMed: 20809529]

Vijayasarathy C, Takada Y, Zeng Y, Bush RA, Sieving PA, 2007. Retinoschisin is a peripheral membrane protein with affinity for anionic phospholipids and affected by divalent cations. Invest Ophthalmol Vis Sci 48, 991–1000. [PubMed: 17325137]

Vijayasarathy C, Zeng Y, Marangoni D, Dong L, Pan ZH, Simpson EM, Fariss RN, Sieving PA, 2022. Targeted Expression of Retinoschisin by Retinal Bipolar Cells in XLRS Promotes Resolution of Retinoschisis Cysts Sans RS1 From Photoreceptors. Invest Ophthalmol Vis Sci 63, 8.

Walia S, Fishman GA, Molday RS, Dyka FM, Kumar NM, Ehlinger MA, Stone EM, 2009. Relation of response to treatment with dorzolamide in X-linked retinoschisis to the mechanism of functional loss in retinoschisin. Am J Ophthalmol 147, 111–115 e111. [PubMed: 18834580]

Wang T, Waters CT, Rothman AM, Jakins TJ, Romisch K, Trump D, 2002. Intracellular retention of mutant retinoschisin is the pathological mechanism underlying X-linked retinoschisis. Hum Mol Genet 11, 3097–3105. [PubMed: 12417531]

Wang T, Zhou A, Waters CT, O'Connor E, Read RJ, Trump D, 2006. Molecular pathology of X linked retinoschisis: mutations interfere with retinoschisin secretion and oligomerisation. Br J Ophthalmol 90, 81–86. [PubMed: 16361673]

Weber BH, Janocha S, Vogt G, Sander S, Ewing CC, Roesch M, Gibson A, 1995. X-linked juvenile retinoschisis (RS) maps between DXS987 and DXS443. Cytogenet Cell Genet 69, 35–37. [PubMed: 7835082]

Weber BH, Schrewe H, Molday LL, Gehrig A, White KL, Seeliger MW, Jaissle GB, Friedburg C, Tamm E, Molday RS, 2002. Inactivation of the murine X-linked juvenile retinoschisis gene, Rs1h, suggests a role of retinoschisin in retinal cell layer organization and synaptic structure. Proc Natl Acad Sci U S A 99, 6222–6227. [PubMed: 11983912]

Weve H, 1938. Ablatio Falciformis Congenita (Retinal Fold). Br J Ophthalmol 22, 456–470. [PubMed: 18169555]

Wu JW, Liu HL, 2012. In silico investigation of the disease-associated retinoschisin C110Y and C219G mutants. J Biomol Struct Dyn 29, 937–959. [PubMed: 22292953]

Wu WW, Molday RS, 2003. Defective discoidin domain structure, subunit assembly, and endoplasmic reticulum processing of retinoschisin are primary mechanisms responsible for X-linked retinoschisis. J Biol Chem 278, 28139–28146. [PubMed: 12746437]

Wu WW, Wong JP, Kast J, Molday RS, 2005. RS1, a discoidin domain-containing retinal cell adhesion protein associated with X-linked retinoschisis, exists as a novel disulfide-linked octamer. J Biol Chem 280, 10721–10730. [PubMed: 15644328]

Yang T-C, Chang C-Y, Yarmishyn AA, Mao Y-S, Yang Y-P, Wang M-L, Hsu C-C, Yang H-Y, Hwang D-K, Chen S-J, Tsai M-L, Lai Y-H, Tzeng Y, Chang C-C, Chiou S-H, 2020. Carboxylated nanodiamond-mediated CRISPR-Cas9 delivery of human retinoschisis mutation into human iPSCs and mouse retina. Acta Biomaterialia 101, 484–494. [PubMed: 31672582]

Zeng Y, Petralia RS, Vijayasarathy C, Wu Z, Hiriyanna S, Song H, Wang YX, Sieving PA, Bush RA, 2016. Retinal Structure and Gene Therapy Outcome in Retinoschisin-Deficient Mice Assessed by Spectral-Domain Optical Coherence Tomography. Invest Ophthalmol Vis Sci 57, OCT277–287.

Zeng Y, Qian H, Campos MM, Li Y, Vijayasarathy C, Sieving PA, 2022. Rs1h(−/y) exon 3-del rat model of X-linked retinoschisis with early onset and rapid phenotype is rescued by RS1 supplementation. Gene Ther 29, 431–440. [PubMed: 34548657]

Zeng Y, Takada Y, Kjellstrom S, Hiriyanna K, Tanikawa A, Wawrousek E, Smaoui N, Caruso R, Bush RA, Sieving PA, 2004. RS-1 Gene Delivery to an Adult Rs1h Knockout Mouse Model Restores ERG b-Wave with Reversal of the Electronegative Waveform of X-Linked Retinoschisis. Invest Ophthalmol Vis Sci 45, 3279–3285. [PubMed: 15326152]

Zhang T, Cheng G, Chen P, Peng Y, Liu L, Li R, Qiu B, 2022. RS1 gene is a novel prognostic biomarker for lung adenocarcinoma. Thorac Cancer 13, 1850–1861. [PubMed: 35569920]

Zhour A, Bolz S, Grimm C, Willmann G, Schatz A, Weber BH, Zrenner E, Fischer MD, 2012. In vivo imaging reveals novel aspects of retinal disease progression in Rs1h(−/Y) mice but no therapeutic effect of carbonic anhydrase inhibition. Vet Ophthalmol 15 Suppl 2, 123–133.

Highlights

- X-linked retinoschisis (XLRS) is characterized by separation of retinal layers (schisis)
- Many mutations in retinoschisin (RS1) cause XLRS and vision loss
- The mutations prevent folding, assembly or secretion, and loss of adhesion between retinal layers
- The cryoEM structures of RS1 provide reasons for deficiencies in mutant expression and function
- How RS1 maintains the integrity of the retina through adhesion remains an open question

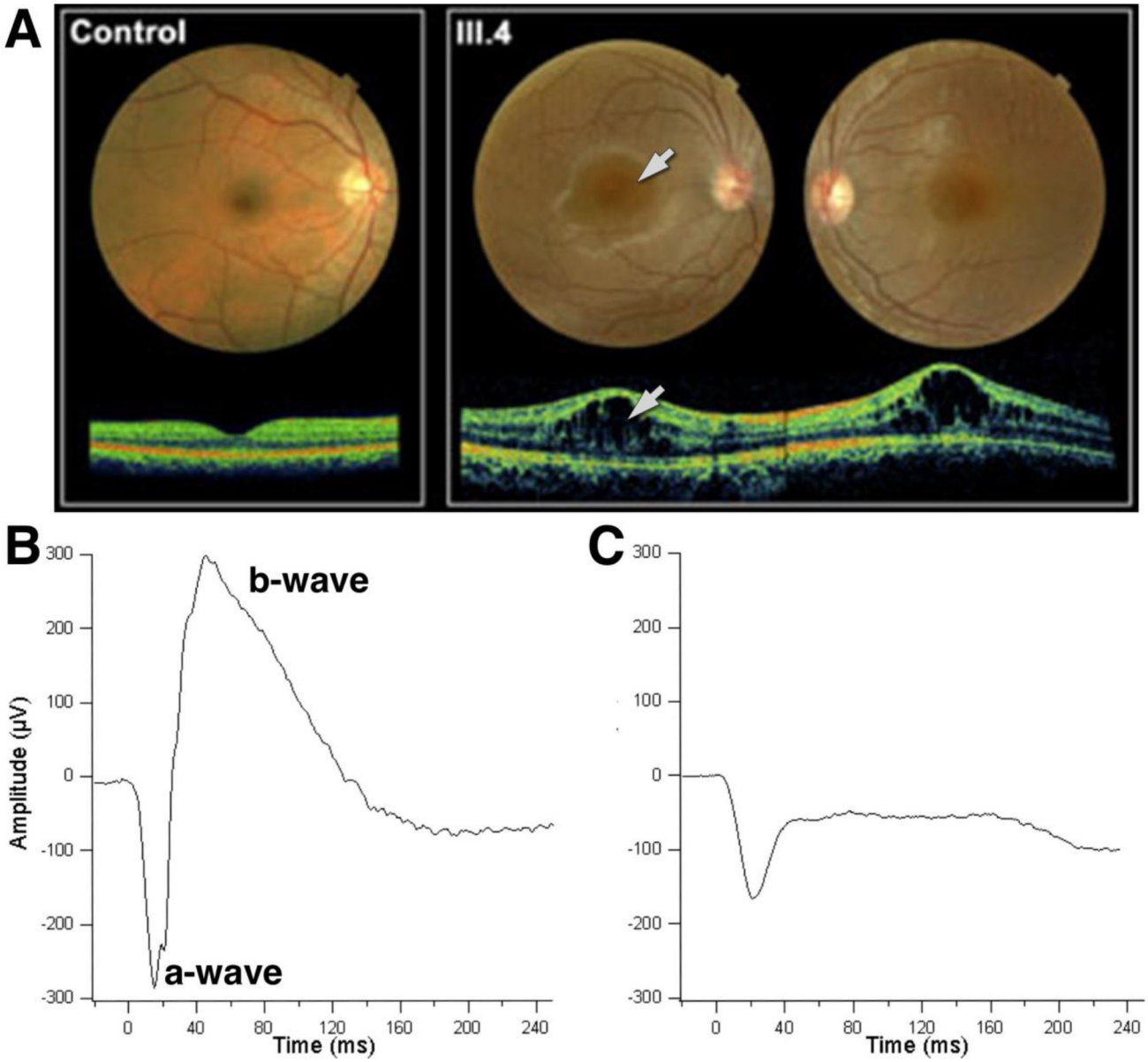

Figure 1:

Diagnostic features of XLRS. (A) Fundus photographs of a normal retina left and the two eyes of a 13 year old patient with XLRS with classical foveal schisis or cysts (arrows). The corresponding spectral domain optical coherence tomograms (SD-OCTs) at the bottom indicate the layered structure of the retinas that is disrupted in XLRS, resulting in separation and the formation of cysts (Vijayasarathy et al., 2010). (B) Electroretinogram (ERG) of a control eye showing the characteristic a- and b-waves. (C) ERG of a diseased eye with a reduced a-wave and suppressed b-wave potential (Bowles et al., 2011).

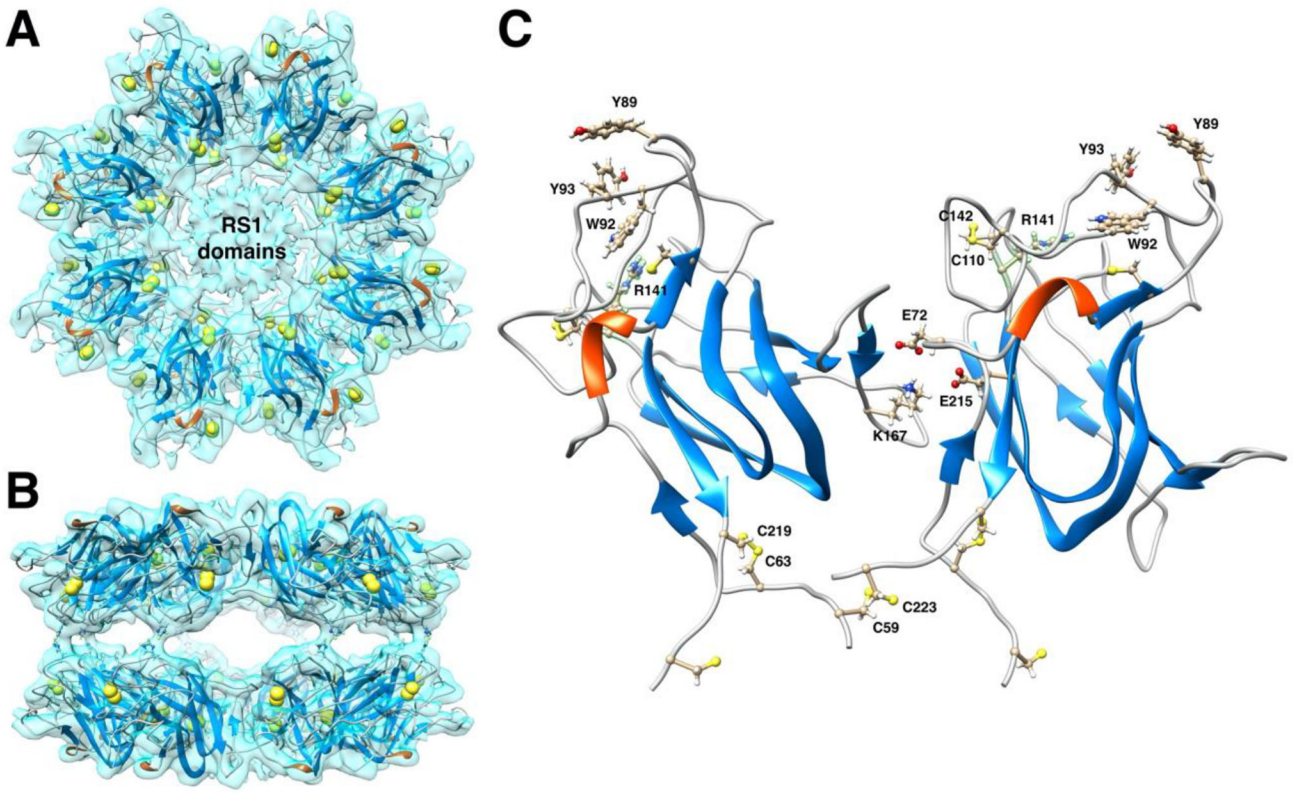

Figure 2:

(A,B) Top and side views of the 16-mer structure of RS1 (Tolun et al., 2016) with disulfide bonds (yellow spheres) crosslinking the subunits internally and between each other in each octameric ring. The RS1 domains occupy the center of each ring but have no ordered structure. (C) Two subunits of RS1 showing important residues where disease-causing mutations occur. Some mutations disrupt proper folding and oligomerization, including disulfide bonds (C59-C223, C63-C219 and C110-C142) and ionic interactions in the subunit interfaces (E72, K167 and E215). Also shown are peripheral residues in the spikes involved in higher order assemblies (Y89, W92 and Y93) and the buried R141, where mutations do not prevent the formation and secretion of the double octamer, but they still cause XLRS.

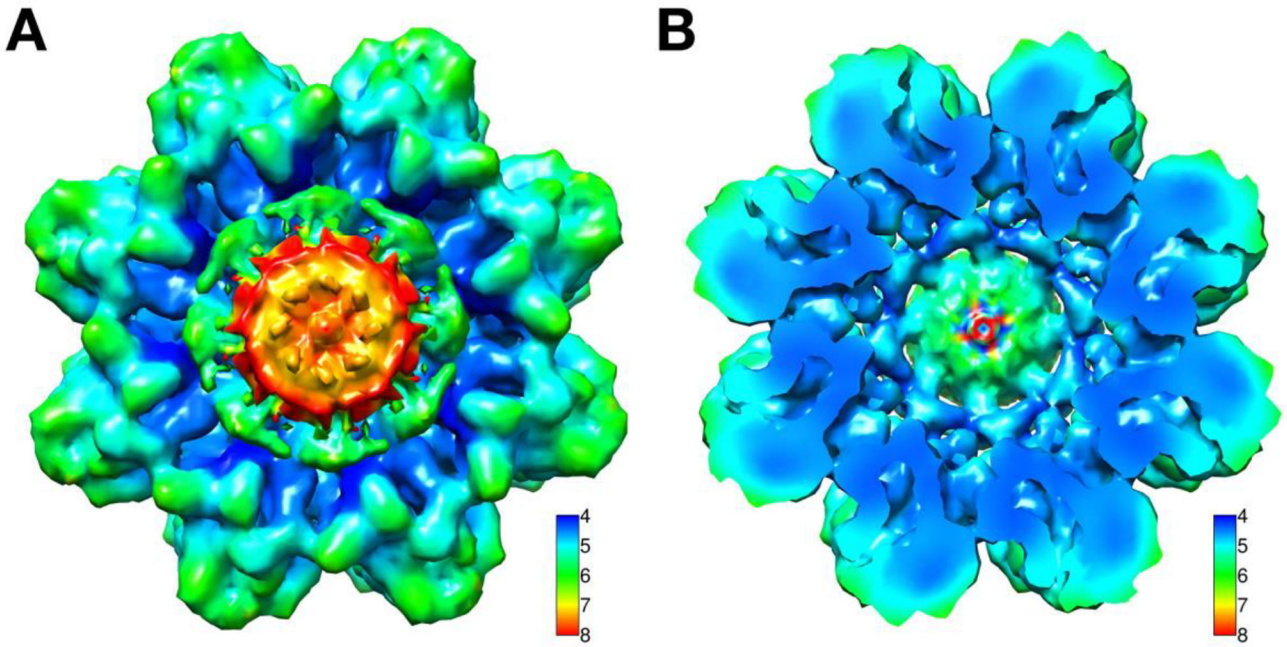

Figure 3:

Comparison of the two cryoEM maps of RS1 using local resolution analysis. (A) The discoidin domain core shows the highest resolution just above 4 Å (blue) while the periphery and the RS1 domain shows the lowest resolution. (B) Cut through the map showing a consistent resolution of 4 Å for the discoidin domain, indicating little difference between the core structures of the two maps.

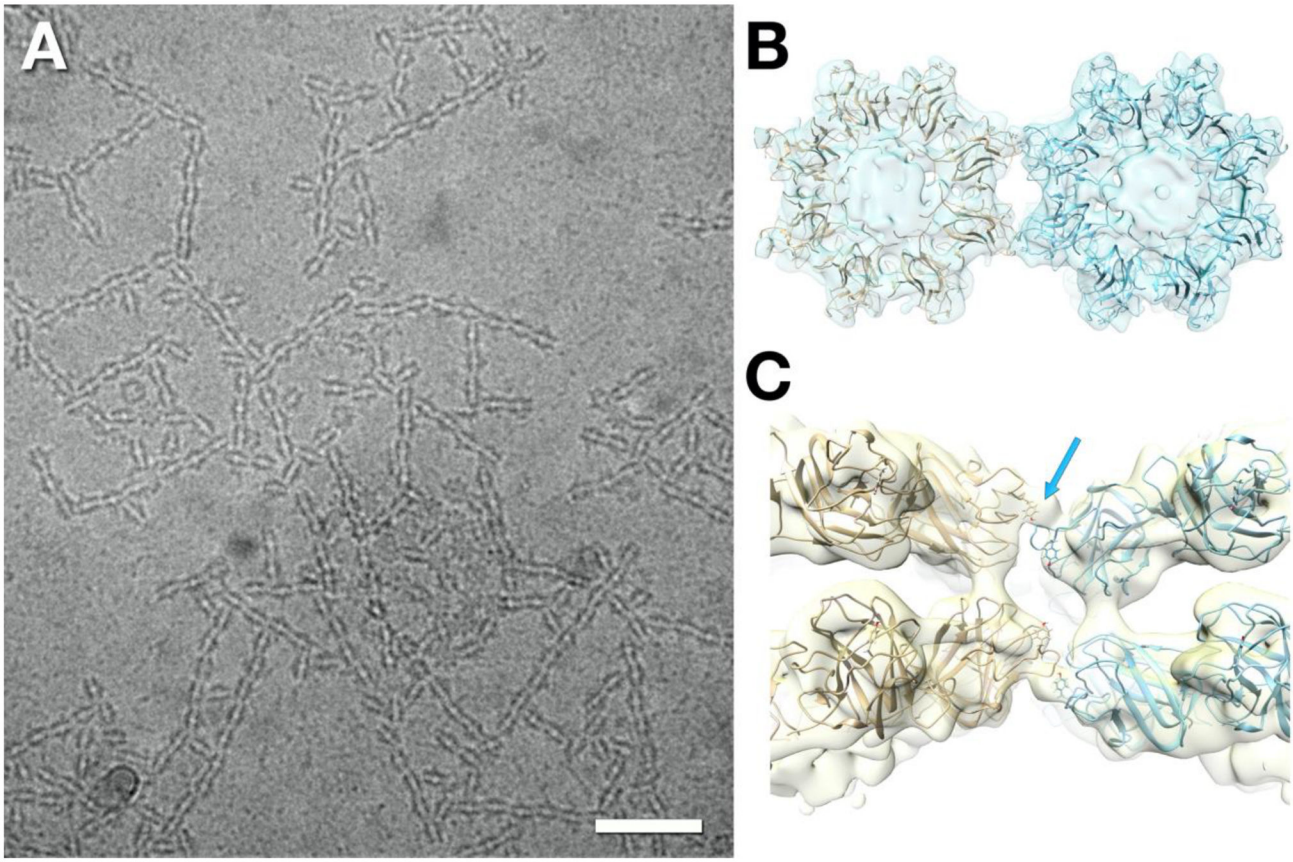

Figure 4:

Higher order assembly of RS1. (A) Under appropriate conditions, RS1 forms filamentous networks. Scale bar: 500 Å. (B) A reconstruction of the major dimer in the filament, indicating that the major interaction is a lateral association of the protruding loops. (C) One loop is particularly prominent in these interactions, containing residues Y89, W92, and Y93 (arrow).

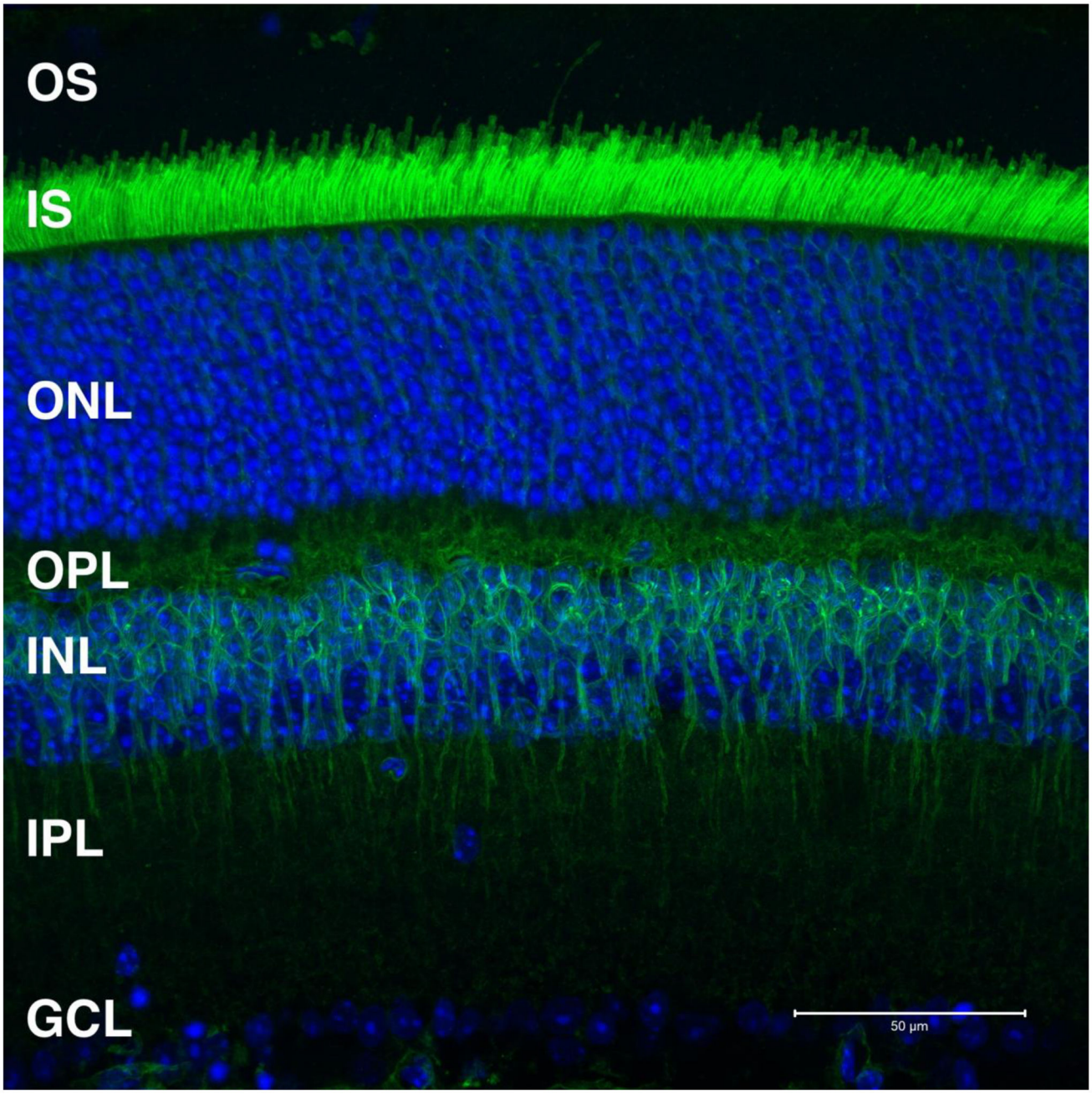

Figure 5:

Confocal immunolocalization of retinoschisin in normal mouse retina. Retinoschisin (green), a secreted protein, localizes most abundantly to the plasma membrane of photoreceptor inner segments (IS) and bipolar cells in the inner nuclear layer (INL). There is some staining in the plexiform layers (OPL and IPL) where most of the synapses are located. Nuclei are labeled with DAPI (blue). The vibratome sections and Airyscan images of aldehyde-fixed mouse retina were prepared as described in Veleri et al. (Veleri et al., 2017). The retina was immunolabeled with an antibody to RS1 + goat anti-rabbit Alexa 488 (green).

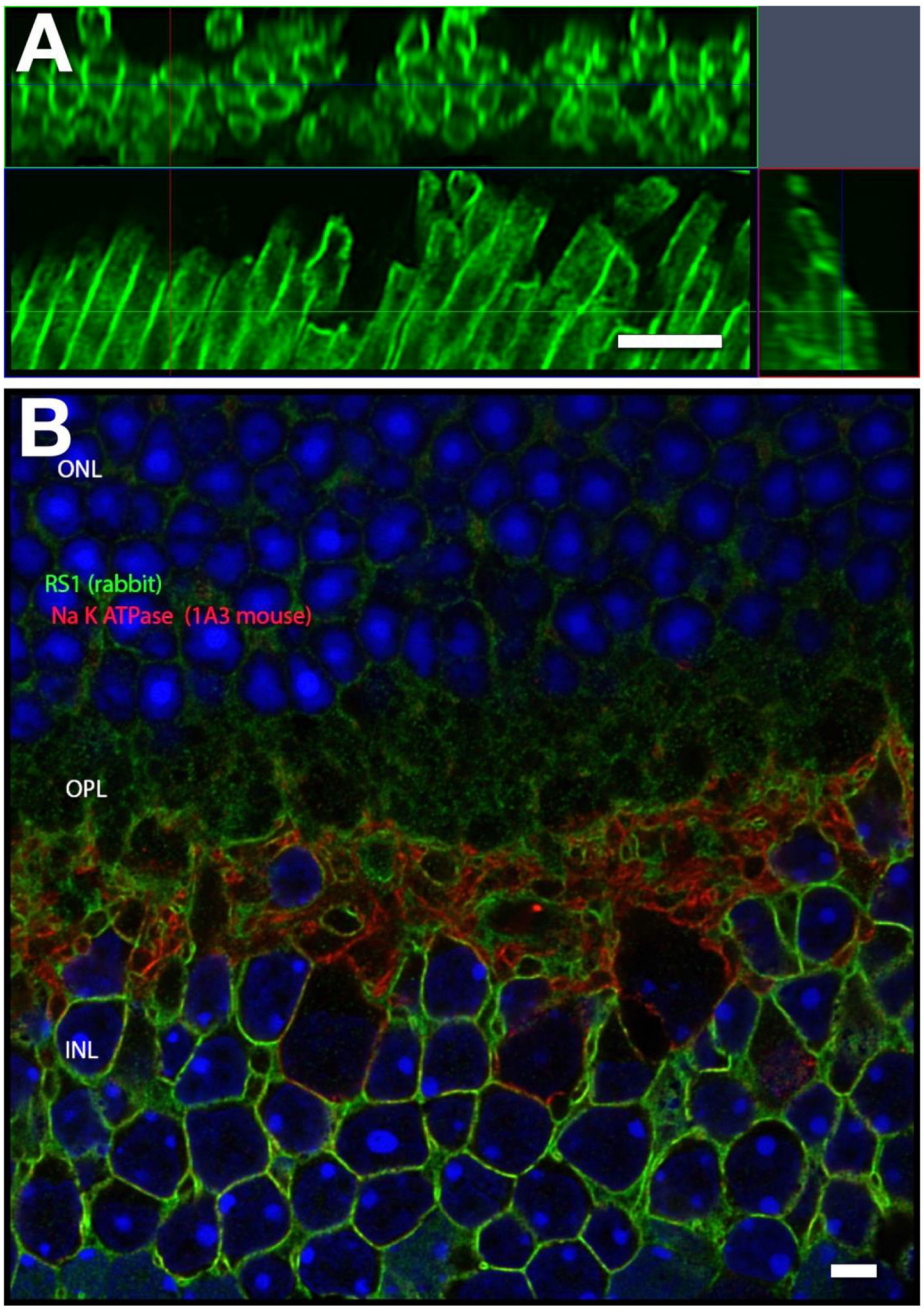

Figure 6:

Airyscan images of RS1 localization (green). (A) Three orthogonal views through the photoreceptors showing RS1 labeling (top panel: end-on view; bottom panels: side views). The membranes of the inner segments (IS) label brightly, while the outer segments (OS) have no discernible label. (B) Longitudinal section of the retina with the photoreceptor nuclei (blue) in the ONL, synapses in the OPL and mostly bipolar cells in the INL. The RS1 labeling is visible on the surfaces of bipolar cell bodies as well as on dendrites projecting into the OPL. The vibratome sections and Airyscan images of aldehyde-fixed mouse retina were prepared as described in Veleri et al. (Veleri et al., 2017). The retina was

immunolabeled with an antibody to RS1 + goat anti-rabbit Alexa 488 (green). Other labeling in (B) included DAPI staining of the cell nuclei (blue) and an antibody to the NaK-ATPase (red) (Vijayasarathy et al., 2022). Scale bars: 2 μm.